Homo- and heteroleptic phototoxic dinuclear metallo-intercalators based on Ruii (dppn) intercalating moieties: synthesis, optical and biological studies.

*Hiwa K. Saeed, Paul J. Jarman, Stuart Archer, Sreejesh Sreedharan, Ibrahim Q Saeed, Luke K. Mckenzie, Julia A Weinstein, Niklaas J Buurma, Carl G. W. Smythe, and Jim A. Thomas**

Abstract: *Using a new mononuclear "building block," for the first time, a dinuclear Ru^{II}(dppn) complex and a heteroleptic system containing both Ru^{II}(dppz) and Ru^{II}(dppn) moieties are reported. The complexes, including the mixed dppz/dppn system, are $^1O_2$ sensitizers. However, unlike the homoleptic dppn systems, the mixed dppz/dppn complex also displays a luminescence "switch on" DNA light-switch effect. In both cisplatin sensitive and resistant human ovarian carcinoma lines the dinuclear complexes show enhanced uptake compared to their mononuclear analogue. Thanks to a favorable combination of singlet oxygen generation and cellular uptake properties all three of the new complexes are phototoxic and display potent activity against chemotherapeutically resistant cells.*

Kinetically inert luminescent metal complexes that interact with biomolecules are now much studied. [1-5] In this context, the photophysics and biomolecular recognition properties of polypyridyl complexes containing the Ru^{II}dppz unit have attracted particular attention, as many of the complexes display a "DNA light-switch" effect, in which Ru→dppz-based ^{3}MLCT emission is "switched on" through DNA intercalation. [6-9] Although the parent complex, $[Ru(N\text{-}N)_2(dppz)]^{2+}$ (where N-N = 2,2'-bipyridyl, 1,10-phenanthroline), displays poor cellular uptake, derivatives that are potential cell imaging probes for optical microscopy have consequently been developed, through increasing lipophilicity or by adding appropriate targeting ligands.[10,11]

Oligonuclear complexes containing Ru^{II}dppz units have also been investigated. In pioneering work, the Nordén and Lincoln groups have reported on the synthesis and biophysical properties of chirally resolved dinuclear complexes tethered through linkers attached to the intercalation site.[12] Due to their distinctive connectivity, these systems are "DNA staples", threading into DNA in a manner similar to naturally occurring molecules such as nogalamycin.[13] Again, these complexes are not spontaneously taken up by live cells, unless their membrane structure is disrupted.[14] The enhanced DNA binding of dinuclear complexes has also been shown by Aldrich-Wright and co-workers, when two optically unresolved $[Ru^{II}(dpq)_2(phen)]$ units (where dpq = dipyrido[3,2-*d*:2',3'-*f*]quinoxaline) are joined together through a flexible 2-mercapto-ethyl ether attached to their non-intercalative phen ligands, which gave DNA binding affinities up to three orders of magnitude higher than their mononuclear analogues.[15] Although subsequent studies on similar systems have been reported, [16] oligonuclear complexes incorporating more extended intercalating moieties are rare, whilst systems containing sites containing different intercalating ligands have not yet been explored.

Photoactive metal complexes have also been investigated as sensitizers for photodynamic therapy, PDT. [17-20] Although Ru^{II}dppz systems for such applications have been reported, [21,22] work on related M(dppn)-based complexes (M= Re^{I}, Ru^{II}, Os^{II}) has gained in significance. [23-26] [27] [28] Unlike their dppz analogues, dppn-based complexes commonly display a dppn-based π→π* excited state that has a lifetime of tens of microseconds and are thus very efficient singlet oxygen sensitizers. [29]

In the context of such studies, we have investigated the properties of achiral $[Ru(tpm)(L)(dppz)]^{2+}$ complexes (where tpm = tris(pyrazolyl)methane, L = a monodentate N-donor ligand). [30,31] These units have provided more facile methods toward the synthesis of oligomeric metallo-intercalators. [32-34] Given the proven therapeutic potential of the Ru^{II}dppn-moiety, we set out to synthesize dinuclear systems that incorporate this unit and, for the first time, the syntheses of both dinuclear homoleptic (Ru^{II}dppn) and heteroleptic (Ru^{II}(dppz)/Ru^{II}(dppn)) complexes are described. In the initial studies reported herein we also compare the photophysical and cell-based biological properties of these new complexes with their Ru^{II}dppz analogues. These studies reveal that the new dppn systems are promising therapeutic and theranostic leads.

Using the complex $[(tpm)Ru(dppn)(Cl)]^+$ and the dipyridyl tether ligand, both prepared using published procedures, [31,34] monomer complex $\mathbf{1}^{2+}$ is readily accessed. Bimetallic complex $\mathbf{2}^{4+}$ could then be prepared through an addition of excess monomer $\mathbf{1}^{2+}$ to a solution of $[(tpm)Ru(dppn)(Cl)^+$ - Fig. 1. In a similar manner, the first dinuclear heteroleptic Ru^{II}dppz/Ru^{II}dppn complex, $\mathbf{3}^{4+}$, was synthesized using the previously reported mono nuclear complex $[(tpm)Ru(dppz)(L1)]^{2+}$, which was reacted with $[(tpm)Ru(dppn)(Cl)]^+$ to yield the required product**.**

[*] Dr H K Saeed, Dr P J Jarman, Dr S Archer, S Sreedharan, L McKenzie, Prof J A Weinstein, Prof J A Thomas
Department of Chemistry
University of Sheffield Sheffield, S3 7HF (UK) E-mail: james.thomas@sheffield.ac.uk

Prof C G W Smythe
Department of Biomedical Science
University of Sheffield
Sheffield, S10 2TN (UK))

Dr I Q Saeed, Dr N J Buurma
Physical Organic Chemistry Centre, School of Chemistry
Cardiff University
Main Building, Park Place, Cardiff, CF10 3AT (UK)

[**] HKS and IQS are grateful to the SKRG-Scholarship "Human Capacity Development Program (HCDP)" for financial support. PJJ and SA are grateful to EPSRC for doctoral funding. SS is grateful to UoS for funding of an *Imaging Life* PhD studentship.

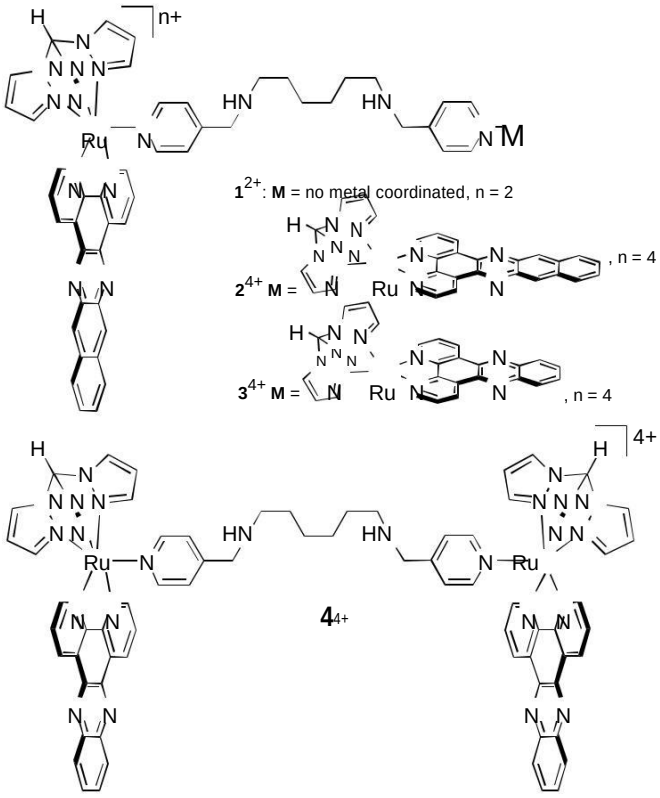

Figure 1. Complexes relevant to this report: $\mathbf{1}^{2+}$ is the mononuclear building block for the synthesis of complexes $\mathbf{2}^{4+}$ and $\mathbf{3}^{4+}$. The synthesis of $\mathbf{4}^{4+}$ has been reported previously.

The photophysical properties of new complexes $\mathbf{1}^{2+}$, $\mathbf{2}^{4+}$ and $\mathbf{3}^{4+}$ as their hexafluorophosphate salts in acetonitrile are summarized in the SI. Apart from intense intraligand (IL) $\pi \rightarrow \pi^*$ transitions at 250 –320 nm, the complexes displayed double humped absorption between ~390 and ~420 nm, which – in comparison to the free ligand – can also be assigned to dppn-based IL transitions. Similarly, since the UV−Vis spectrum of the dppz ligand in acetonitrile displays a moderately intense IL band with two principal maxima at λ = 358 and 376 nm, the intense band at 361 nm observed in the spectrum of complex $\mathbf{3}^{4+}$ is assigned to a $\pi \rightarrow \pi^*$(dppz) transition. Bands observed at 450 - 490 nm are assigned as MLCT transitions as these typically occur at this energy in these complexes. As expected from previous studies, complexes $\mathbf{1}^{2+}$ and $\mathbf{2}^{4+}$ - which only contain Ru^{II}dppn units - are not luminescent. In contrast, complex $\mathbf{3}^{4+}$ *does* display a broad emission centered at 644 nm, which is typical of Ru→dppz ^{3}MLCT-based luminescence.

To investigate the photo-excited state of the new dinuclear complexes in more detail, preliminary transient absorption studies in acetonitrile were carried out. The transient difference spectra obtained in flash photolysis experiments for $\mathbf{2}^{4+}$ and $\mathbf{3}^{4+}$ are shown in Figure 2 where they are compared to the data obtained with homoleptic dinuclear complex Ru^{II}dppz complex $\mathbf{4}^{4+}$. For completeness, mononuclear complexes $\mathbf{1}^{2+}$ and its Ru^{II}dppz analogue were also studied using this technique (see SI Fig 1).

Excitation of all three complexes using a 7 ps laser pulse at 355 nm, measured over a time window of 3.5 nanoseconds, leads to the formation of several transient bands due to ground state bleaching – Fig 2. The transient spectra for the three complexes are unmatched, implying that the excited state accessed on the picosecond time scale is not the same in each case. As expected, the observed transient spectrum of complex $\mathbf{4}^{4+}$ (Fig 2A) and mononuclear analogue (see SI), shows a broad absorption at ~600 nm, indicating occupation of the Ru→dppz-based ^{3}MLCT state. However, the transient absorption spectrum of complex $\mathbf{2}^{4+}$ (Fig 2B) differs significantly from that of $\mathbf{4}^{2+}$ and is consistent with an expected dppn-based $^3\pi\pi^*$state, which displays an absorption at ~540 nm; [29] comparable to its mononuclear analogue $\mathbf{1}^{2+}$, which displays a similar trace (see SI).

Interestingly, the transient absorption spectrum of complex $\mathbf{3}^{4+}$ (Fig 2C), which contains both dppz/dppn ligands, is a combination of the individual excited states observed for $\mathbf{2}^{4+}$ and $\mathbf{4}^{4+}$. The structured $^3\pi\pi^*$ absorption grows in at 540 nm accompanied by the broad ^{3}MLCT absorption around ~600 nm, indicating that – at least on this timescale – both excited states are occupied. More detailed studies on the evolution of these excited states over longer time windows are currently underway and will be reported in a future report.

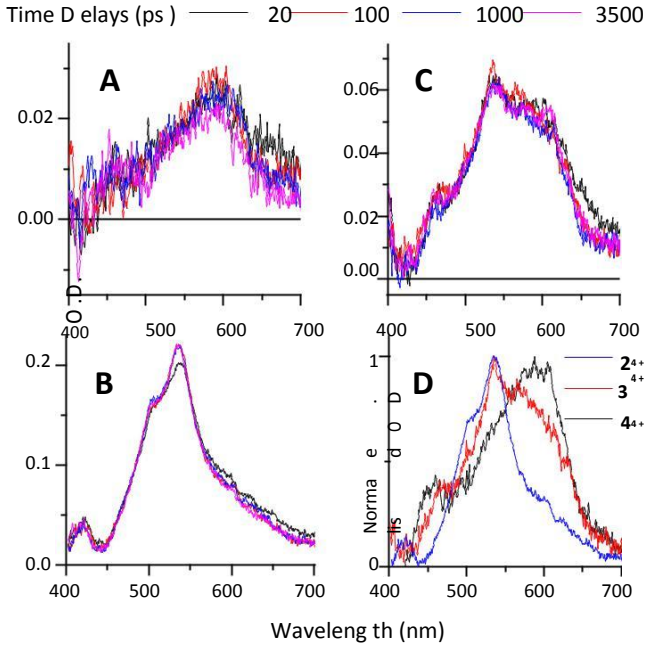

Figure 2. Transient absorption spectra for dinuclear complexes $\mathbf{4}^{4+}$ (A), $\mathbf{2}^{4+}$ (B), $\mathbf{3}^{4+}$ (C) recorded in acetonitrile at selected time delays. The normalised excited states at 100 ps for all complexes is shown in panel D for comparison - **2** and **3** are shown at 100 ps, the spectrum for **4** has been summed between 30-200 ps to improve signal-to-noise, as no spectral changes are observe during this timescale.

Photoexcitation of complexes containing the Ru^{II}dppn unit have been found to sensitize singlet oxygen, with yields of >70 % being achieved. Consequently, the sensitization properties of the three new complexes were assessed by the direct measurement of $O_2(^1\Delta_g) \rightarrow {}^3O_2$ phosphorescence at 1270 nm and compared to data obtained for complex $\mathbf{4}^{4+}$ - Table 1.

The data for the complexes clearly illustrate that access to the $^3\pi\pi^*$ state of the dppn ligand does increase sensitization. Dinuclear complex $\mathbf{4}^{4+}$ is a poor $^1O_2$ sensitizer, displaying properties that are comparable to many mononuclear Ru^{II}dppz systems. [35] In contrast, complexes $\mathbf{1}^{2+}$ and $\mathbf{2}^{4+}$ are efficient sensitizers, so that their $^1O_2$ quantum yields are up to 13-fold higher than $\mathbf{4}^{4+}$. Although complex $\mathbf{3}^{4+}$ incorporates the Ru^{II}dppn unit and does photo-generate $^1O_2$ at higher levels than $\mathbf{4}^{4+}$, it is a poorer sensitizer than $\mathbf{1}^{2+}$ and $\mathbf{2}^{4+}$. This

observation is again consistent with occupation and equilibration between the $^3\pi\pi^*$ state and the shorter lived Ru^{II}dppz ^{3}MLCT state. Indeed we have observed a similar phenomenon in a related heteronuclear Ru^{II}dppz/Re^{I}dppz system, in which the ^{3}MLCT of the Ru^{II} centre interacts with the $^3\pi\pi^*$ dppz-based excited state of the Re^{I}dppz unit.

Table 1. Singlet oxygen yield on irradiation of complexes $\mathbf{1}^{2+}$, $\mathbf{2}^{4+}$ and $\mathbf{3}^{4+}$ and $\mathbf{4}^{4+}$[a]

Complex	$^1O_2$ yield %
$\mathbf{1}^{2+}$	59.3 (± 2)
$\mathbf{2}^{4+}$	67.2 (± 5)
$\mathbf{3}^{4+}$	15.7 (± 1)
$\mathbf{4}^{4+}$	4.9 (± 1)

[a] Recorded in acetonitrile using hexafluorophosphate salts.

Water-soluble chloride salts of all three new complexes were obtained *via* anion metathesis of their respective PF_6^- salts using [*n*Bu4N]Cl in acetone. Their interaction with CT-DNA in aqueous buffer (25 mM NaCl, 5 mmol tris, pH 7.0) was first investigated using UV–visible spectroscopic titrations. Addition of CT-DNA results in characteristically large hypochromicity in both MLCT and π→π* absorption bands, producing typical saturation binding curves - see Fig. 4. As previously reported for systems such as $\mathbf{4}^{4+}$, attempts to fit titration data to the well-known McGhee-Von Hippel model[36] for non-cooperative binding proved unsuccessful. As in previous studies, despite the sequence heterogeneity of CT-DNA, absorption spectroscopic titrations could be reproduced by a multiple independent binding sites, MIS, model, [37] which explicitly takes the ligand concentration into account, and thus avoids the need to keep the ligand concentration constant upon addition of DNA – See SI. The binding parameters derived from these fits are summarized in Table 2. To aid comparisons, the binding affinity for $\mathbf{4}^{4+}$ estimated using the same methods are included.

Table 2. Estimates of binding constants for complexes relevant to this study obtained from fits the MIS model to UV-Visible titrations [a]

Complex	K_b / 10^5 M^{-1}	binding site / b.p.	ε_{MLCT} / 10^4 M^{-1} cm^{-1}	ε_{MLCT} / 10^4 M^{-1} cm^{-1}
$\mathbf{1}^{2+}$	12.2±3.5	0.99±0.03	3.48±0.02	-1.62±0.03
$\mathbf{2}^{4+}$	1.1±0.3	1.0±0.1	3.46±0.02	-1.66±0.04
$\mathbf{3}^{4+}$	1.7±0.7	2.6±0.1	9.04±0.02	-7.1±0.7
$\mathbf{4}^{4+}$	8.9	0.85	6.43	-3.77

[a] Fit of the MIS model (described in Ref 37) to data from UV-visible titrations. Conditions: 25mM NaCl, 5mM Tris-HCl, pH 7.4, 25°C.

In fluorescence titrations, as expected, both $\mathbf{1}^{2+}$, and $\mathbf{2}^{4+}$ showed no emission in aqueous solution, even upon addition of CT-DNA. These observations are consistent with previous reports, and with our studies on the hexafluorophosphate salts, indicating that the lowest excited state of the Ru^{II}dppn moiety is the non-emissive dppn-based π→π* state. In contrast, $\mathbf{3}^{4+}$ displays increasing emission upon progressive addition of CT-DNA. The fact that a distinctive DNA light switch effect is observed is in agreement with the transient absorption studies and confirms that the Ru(dπ)→dppz (π*) ^{3}MLCT excited state of complex $\mathbf{3}^{4+}$ is occupied.

For all new complexes, binding thermodynamics with DNA at 25 °C were determined by ITC. Their heat of dilutions were found to be constant, indicating that they do not aggregate under the experimental conditions; consequently, titrations with CT-DNA were then carried out. Typical enthalpograms for these titrations are shown in the SI. Potential binding models were explored by fitting a model involving two different DNA-ligand binding events to the calorimetric data using the I2CITC software package[38,39] with the corresponding parameters K_A, H_A, n_A, (for equilibrium A), K_B, H_B and n_B (for equilibrium B) all optimised without restrictions. The merit of these binding models was evaluated through analysis of the covariance between the stoichiometries n_A and n_B, in combination with whether suggested binding site sizes are reasonable (See SI for details). This analysis highlighted a common binding event involving a binding site of six to seven base pairs for all complexes three complexes. The calorimetry data were therefore re-analysed, restricting the first binding site size to 7.5 basepairs and 6.2 basepairs for $\mathbf{1}^{2+}$ and $\mathbf{2}^{4+}$, respectively. For $\mathbf{3}^{4+}$, the data were re-analysed in terms of a model involving one binding site. The resulting thermodynamic parameters as summarized in Table 3 shows that the high affinity binding modes of complexes are very similar in binding site and affinity. The stoichiometry for the secondary binding events suggests that this involves non-specific binding, potentially through electrostatic interactions. Remarkably, $\mathbf{3}^{4+}$ does not seem to display a secondary binding event of sufficient strength to be noticeable in the calorimetric data. Any differences in affinity and binding site size according the UV-visible titrations and ITC experiments is likely the result of the presence of different types of binding sites on the DNA, which is not reproduced by the MIS model.

Table 3. Estimates of binding constants for complexes relevant to this study obtained from fits the MIS model to UV-Visible titrations [a,b]

parameter	$\mathbf{1}^{2+}$	$\mathbf{2}^{4+}$	$\mathbf{3}^{4+}$
K_A / M^{-1}	1.8×10^6	2.8×10^6	1.5×10^6
n_A / b.p.	7.5[c]	6.2 [c]	5.9
H_A / kJ mol^{-1}	-0.5	2.1	10.6
K_B / M^{-1}	1.2×10^5	1.6×10^5	---
n_B / b.p.	2.17	2.43	---
H_B / kJ mol^{-1}	2.8	4.8	---

[a] Conditions: 25mM NaCl, 5mM Tris-HCl, pH 7.4, 25°C. [b] For confidence intervals, see the SI [c] Binding site size restricted following binding model exploration.

Although $\mathbf{1}^{2+}$ and $\mathbf{2}^{4+}$ are non-emissive, since complex $\mathbf{3}^{4+}$ is luminescent its cell uptake properties were investigated using wide-field fluorescence microscopy. It was found that after just 15 minutes exposure to [**3**]Cl_4, even at concentrations as low as 20 μM, uptake into live A2780 cells could be clearly observed through its characteristic ^{3}MLCT-based emission. Although the complex binds to DNA in cell free conditions, it is clear that, within live cells, $\mathbf{3}^{4+}$ produces negligible nuclear staining; however, bright emission from specific regions within the cytoplasm is observed. To investigate this issue further, cells were co-stained with organelle specific luminescent probes.

Lipophilic cations often accumulate within mitochondria,[40] therefore initial co-localisation experiments involved the commercial probe mitotracker deep red, MTDR. As observed in Fig 3A, although it is clear that there is some overlap between the emission of MTDR and $\mathbf{3}^{4+}$ - confirming that it partly localizes within mitochondria on live cell uptake - a greater correlation is

observed with lysotracker deep red (LTDR), a probe used to label and track acidic lysosomes in live cells, Fig 3B.

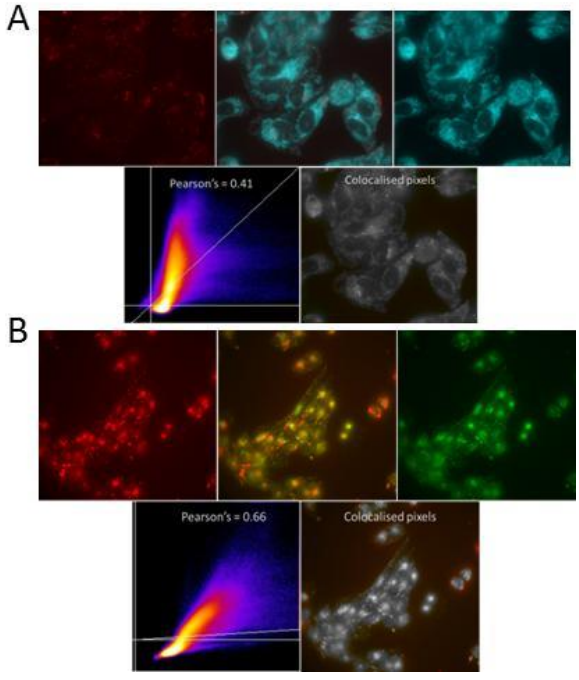

Figure 3. Colocalisation studies involving [**3**]Cl_4. A. Co-localisation study using mitotracker deep red (MTDR). Top left: emission from [[**3**]Cl_4, Top right: emission from MTDR, Top middle: merged images. Bottom Right: colocalised pixels Bottom Left: overlap micrograph. B. Co-localisation study using lysotracker deep red (LTDR). Top left: emission from [**3**]Cl_4, Top right: emission from LTDR, Top middle: merged images. Bottom Right: colocalised pixels Bottom Left: overlap micrograph.

Moreover, homoleptic complex $\mathbf{2}^{4+}$ is taken up into cells with an almost tenfold increase in terms of molarity over heteroleptic complex $\mathbf{3}^{4+}$, producing intracellular concentrations that are considerably higher than the external exposure concentration – Table 5. The higher uptake of the dinuclear complexes is consistent from our previous studies on photo-active metallomacrocycles,[41] which indicated that overall charge density/lipophilicity of the oligonuclear systems can be lower than that of analogous mononuclear complex. The difference in uptake between $\mathbf{2}^{4+}$ and $\mathbf{3}^{4+}$ is also explained by this trend as, overall, $\mathbf{2}^{4+}$ has a larger total aromatic surface relative to $\mathbf{3}^{4+}$.

Table 5. Intracellular metal content (ruthenium) data from ICP-MS analysis.[a]

Complex	Intracellular concentration (μM/L, 24 hours)
$\mathbf{1}^{2+}$	8.6
$\mathbf{2}^{4+}$	1.1×10^3
$\mathbf{3}^{4+}$	1.2×10^2

[a] Conditions: A2780cis treated with 50 μM concentrations of each complex.

Since $\mathbf{1}^{2+}$ and $\mathbf{2}^{4+}$ are non-emissive their uptake in the human ovarian cancer cell line, A2780cis over a 24 hours period was also directly measured and compared to that of $\mathbf{3}^{4+}$ using inductively coupled plasma mass spectrometry (ICP-MS). This analysis revealed that, even allowing for the fact that $\mathbf{2}^{4+}$ and $\mathbf{3}^{4+}$ are dinuclear, the intracellular accumulation of both dinuclear ruthenium complexes are notably higher than that of $\mathbf{1}^{2+}$.

In terms of possible therapeutic applications of these complexes, localization within these organelles rather than the nucleus is particularly advantageous. PDT sensitizers localized in both mitochondria[42,43] and lysosomes[44,45] have been shown to rapidly and efficiently induce apoptosis; [46] indeed, it has been pointed out that $^1O_2$ sensitizers that target nuclear DNA may potentially produce deleterious mutations in any cells that survive treatment. [45] Therefore, given their attractive combination of biomolecular recognition properties and singlet oxygen sensitization, the *in cellulo* phototoxicity of the new complexes were investigated

The potential of the new complexes as PDT sensitizers was investigated using the cisplatin sensitive human ovarian cancer cell line, A2780 and its treatment resistant analogue A2780cis. Cells were exposed to broad-spectrum irradiation in the absence and presence of each complex, using previously described apparatus and protocols. [41] A concentration range of 1 – 100 μM of each complex was used resulting in distinct phototoxic effects that are summarized in Table 6. In the A2780 cell line, even at low concentrations (10 μM) and light fluences (7.5 Jcm^{-2}), both complexes $\mathbf{1}^{2+}$ and $\mathbf{2}^{4+}$ produce rapid decreases in cell viability, leading to nearly total cell death. Comparing dark IC_{50} values to those obtained at 15 Jcm^{-2} light fluence reveals a considerable phototoxic response, particularly for dinuclear complex $\mathbf{2}^{4+}$, which displays a phototoxic index, PI, of >200. Interestingly, although the mixed dppz/dppn system complex $\mathbf{3}^{4+}$ does not show such a large effect, it does still induce a noticeable decrease in cell viability at higher concentrations and light exposure.

Table 6. IC_{50} (μM) for A2780 and A2780cis (in brackets) cells exposed to complexes $\mathbf{1}^{2+}$, $\mathbf{2}^{4+}$, and $\mathbf{3}^{4+}$ as chloride salts upon photoirradiation [a]

	Fluence ($J\,cm^{-2}$)			
Complex	0	7.5	15	PI
$\mathbf{1}^{2+}$	32(>100)	4(1.6)	2(<0.1)	16 (≥1000)
$\mathbf{2}^{4+}$	20(50)	3(3)	<0.1(<0.1)≥200(≥500)	
$\mathbf{3}^{4+}$	60(100)	50(25)	20(7)	3(≥14)

[a] Phototoxic index for irradiation with 15 Jcm^{-2}.

Strikingly, the therapeutically resistant A2780cis cell-line displays greater photosensitivity towards all three complexes compared to its cisplatin sensitive analogue, with PIs up to and over x1000 being observed. Although complex $\mathbf{3}^{4+}$ again induces lower phototoxic effects compared to $\mathbf{1}^{2+}$ and $\mathbf{2}^{4+}$, an appreciable PI of >14 is observed, even with fluences as low as 15 Jcm^{-2}.

In conclusion, the first reported dinuclear homoleptic (Ru^{II}dppn) and heteroleptic (Ru^{II}(dppz)/Ru^{II}(dppn)) complexes display considerable capacity to photogenerate singlet oxygen. Although cell-free studies showed the new complexes bind to DNA and biological studies revealed that - unlike their homoleptic Ru^{II}(dppz) analogue - the complexes were taken up live cells, imaging of luminescent complex $\mathbf{3}^{4+}$ show that it accumulates in mitochondria and especially lysosomes and not in the nucleus. Both mononuclear complex $\mathbf{1}^{2+}$ and homoleptic dinuclear complex $\mathbf{2}^{4+}$ show higher phototoxic indices against cisplatin insensitive A2780cis cells, and display high phototoxic indices; given the increased phototoxicity

against drug resistant cells these complexes are particularly promising therapeutic leads. Although complex $\mathbf{3}^{4+}$ shows a comparatively lower PI, it is still active whilst also displaying luminescence, suggesting that it is a lead for the development of theranostics that could both image and treat solid cancers. Further studies into the therapeutic potential of these complexes and their derivatives will be outlined in future studies.

Experimental Section

See SI for details of experimental and synthetic methods.

Keywords: Ruthenium(II) · PDT · Luminescence · ITC · singlet oxygen

[1] C. P. Montgomery, B. S. Murray, E. J. New, R. Pal, D. Parker, *Acc. Chem. Res.* **2009**, *42*, 925–937.
[2] E. Baggaley, J. A. Weinstein, J. A. Williams, *Coord. Chem. Rev.* **2012**, *256*, 1762–1785.
[3] D.-L. Ma, V. P.-Y. Ma, D. S.-H. Chan, K.-H. Leung, H.-Z. He, C.-H. Leung, *Coord. Chem. Rev.* **2012**, *256*, 3087–3113.
[4] J. A. Thomas, *Chem Soc Rev* **2015**, *44*, 4494–4500.
[5] K. K.-W. Lo, *Acc. Chem. Res.* **2015**, *48*, 2985–2995.
[6] A. E. Friedman, J. C. Chambron, J. P. Sauvage, N. J. Turro, J. K. Barton, *J. Am. Chem. Soc.* **1990**, *112*, 4960–4962.
[7] B. M. Zeglis, V. C. Pierre, J. K. Barton, *Chem. Commun.* **2007**, 4565–4579.
[8] M. R. Gill, J. A. Thomas, *Chem Soc Rev* **2012**, *41*, 3179–3192.
[9] G. Li, L. Sun, L. Ji, H. Chao, *Dalton Trans* **2016**, *45*, 13261– 13276.
[10] C. A. Puckett, J. K. Barton, *J. Am. Chem. Soc.* **2007**, *129*, 46–47.
[11] C. A. Puckett, R. J. Ernst, J. K. Barton, *Dalton Trans* **2010**, *39*, 1159.
[12] B. Önfelt, P. Lincoln, B. Nordén, *J. Am. Chem. Soc.* **1999**, *121*, 10846–10847.
[13] B. Önfelt, P. Lincoln, B. Nordén, *J. Am. Chem. Soc.* **2001**, *123*, 3630–3637.
[14] B. Önfelt, L. Göstring, P. Lincoln, B. Nordén, A. Onfelt, *Mutagenesis* **2002**, *17*, 317–320.
[15] J. Aldrich-Wright, C. Brodie, E. C. Glazer, N. W. Luedtke, L. Elson-Schwab, Y. Tor, *Chem. Commun.* **2004**, 1018.
[16] P. Liu, B.-Y. Wu, J. Liu, Y.-C. Dai, Y.-J. Wang, K.-Z. Wang, *Inorg Chem* **2016**, *55*, 1412–1422.
[17] J. P. Celli, B. Q. Spring, I. Rizvi, C. L. Evans, K. S. Samkoe, S. Verma, B. W. Pogue, T. Hasan, *Chem. Rev.* **2010**, *110*, 2795–2838.
[18] J. D. Knoll, C. Turro, *Coord Chem Rev* **2015**, *282-283*, 110–126.
[19] C. Mari, M. Kaur, S. Ladouceur, G. Gasser, *Chem. Sci.* **2015**, *6*, 2660–2686.
[20] G. Shi, S. Monro, R. Hennigar, J. Colpitts, J. Fong, K. Kasimova, H. Yin, R. DeCoste, C. Spencer, L. Chamberlain, et al., *Coord. Chem. Rev.* **2015**, *282-283*, 127–138.
[21] C. Mari, M. Kaur, C. Agarwal, M. Patra, J. Hess, B. Spingler, L. Oehninger, J. Schur, I. Ott, L. Salassa, et al., *Chem. Eur. J.* **2014**, *20*, 14421–14436.
[22] M. Kaur, C. Agarwal, C. Gentili, M. Patra, C. Mari, G. Gasser, S. Ladouceur, *Chem. Sci.* **2016**, *7*, 6115–6124.
[23] V. W.-W. Yam, K. K.-W. Lo, K.-K. Cheung, R. Y.-C. Kong, *J. Chem. Soc., Chem. Commun.* **1995**, 1191–1193.
[24] Y. Sun, L. E. Joyce, N. M. Dickson, C. Turro, *Chem. Commun.* **2010**, *46*, 2426.
[25] Y. Sun, L. E. Joyce, N. M. Dickson, C. Turro, *Chem. Commun.* **2010**, *46*, 6759.
[26] H. Yin, M. Stephenson, J. Gibson, E. Sampson, G. Shi, T. Sainuddin, S. Monro, S. A. McFarland, *Inorg Chem* **2014**, *53*, 4548–4559.
[27] B. A. Albani, B. Peña, N. A. Leed, N. A. B. G. de Paula, C. Pavani, M. S. Baptista, K. R. Dunbar, C. Turro, *J. Am. Chem. Soc.* **2014**, *136*, 17095–17101.
[28] T. Sainuddin, J. McCain, M. Pinto, H. Yin, J. Gibson, M. Hetu, S. A. McFarland, *Inorg Chem* **2016**, *55*, 83–95.
[29] S. P. Foxon, M. A. H. Alamiry, M. G. Walker, A. J. H. M. Meijer, I. V. Sazanovich, J. A. Weinstein, J. A. Thomas, *J. Phys. Chem. A* **2009**, *113*, 12754–12762.
[30] C. Metcalfe, H. Adams, I. Haq, J. A. Thomas, *Chem. Commun.* **2003**, 1152–1153.
[31] S. P. Foxon, C. Metcalfe, H. Adams, M. Webb, J. A. Thomas, *Inorg Chem* **2007**, *46*, 409–416.
[32] C. Metcalfe, I. Haq, J. A. Thomas, *Inorg Chem* **2004**, *43*, 317–323.
[33] S. P. Foxon, T. Phillips, M. R. Gill, M. Towrie, A. W. Parker, M. Webb, J. A. Thomas, *Angew. Chem. Int. Ed.* **2007**, *46*, 3686– 3688.
[34] H. K. Saeed, I. Q. Saeed, N. J. Buurma, J. A. Thomas, *Chem. Eur. J.* **2017**, *23*, 5467–5477.
[35] C. C. Sentagne, J. C. J. Chambron, J. P. J. Sauvage, N. N. Paillous, *J Photochem Photobiol B* **1994**, *26*, 165–174.
[36] J. D. J. McGhee, P. H. P. von Hippel, *J. Mol. Biol.* **1974**, *86*, 469–489.
[37] L. Hahn, N. J. Buurma, L. H. Gade, *Chem. Eur. J.* **2016**, *22*, 6314–6322.
[38] N. J. Buurma, I. Haq, *Methods* **2007**, *42*, 162–172.
[39] N. J. Buurma, I. Haq, *J. Mol. Biol.* **2008**, *381*, 607–621.
[40] M. P. Murphy, *BBA-Bioenergetics* **2008**, *1777*, 1028–1031.
[41] M. G. Walker, P. J. Jarman, M. R. Gill, X. Tian, H. Ahmad, P. A. N. Reddy, L. McKenzie, J. A. Weinstein, A. J. H. M. Meijer, G. Battaglia, et al., *Chem. Eur. J.* **2016**, *22*, 5996–6000.
[42] M. R. Detty, S. L. Gibson, S. J. Wagner, *J. Med. Chem.* **2004**, *47*, 3897–3915.
[43] R. Hilf, *J Bioenerg Biomembr* **2007**, *39*, 85–89.
[44] M. Dickerson, Y. Sun, B. Howerton, E. C. Glazer, *Inorg Chem* **2014**, *53*, 10370–10377.
[45] H. Huang, B. Yu, P. Zhang, J. Huang, Y. Chen, G. Gasser, L. Ji, H. Chao, *Angew. Chem. Int. Ed.* **2015**, *54*, 14049–14052.
[46] P. Agostinis, K. Berg, K. A. Cengel, T. H. Foster, A. W. Girotti, S. O. Gollnick, S. M. Hahn, M. R. Hamblin, A. Juzeniene, D. Kessel, et al., *CA Cancer J Clin* **2011**, *61*, 250–281.